



Dynamic response of spar platform subjected to far-field underwater shock

E. Salajegheh¹, J. Salajegheh², M. Biglarkhani³

1,2- Department of Civil Engineering, Shahid Bahonar University of Kerman, Iran

3- Department of Civil Engineering, Islamic Azad University of Kerman, Iran

m.biglarkhani@yahoo.com

Abstract

The exploitation of hydrocarbon reservoirs under the seabed in very deep water requires the use of innovative floating platform configurations. The hydrodynamic interaction of such platforms with underwater explosion shock and the understanding and quantification of the dynamic response of these interactions has been a subject of continuing research. This paper examines these dynamic responses for a specific very deep draft spar platform type that is increasingly being used in the oceans. A spar platform must be safe due to underwater shock. The dynamic response of spar platform to underwater shock is very complex. A complete analysis of the problem must involve simultaneous solution of the dynamic response of structure and the propagation of shock wave in surrounding fluid, which makes such general analysis prohibitively expensive. To alleviate the difficulty a method is proposed for a typical spar platform. An explicit method was conducted using finite element based coupled structure and fluid model. In this research for the first time dynamic behavior of typical spar platforms is investigated by underwater explosion models. The results of this research can be used for design of spars against time dependent load such as wind, wave, earthquake and similar forces.

Key world: Dynamic response, Spar platform, Underwater shock, Fluid - Structure interaction

Introduction

As the offshore industry depletes hydrocarbon reservoirs below the sea bed in small to moderate water depths (up to 500 m), it is increasingly required to develop such deposits in considerably deeper water. The high water depth makes the use of sea bed mounted platforms uneconomic leaving a variety of floating platform types as the only viable options for oil and gas production operations. Spar platforms being one such compliant offshore floating structure used for deep water applications for the drilling, production, processing, storage and offloading of ocean deposits. It is being considered the next generation of deep water offshore structures by many oil companies. It consists of a very large floating vertical cylindrical structure of around 250 m draft and 40 m or so in diameter, depending on its application and the environment in which it works [1]. The structure floats so deep in the water that the wave action at the surface is dampened by the counter balance effect of the structure weight. Station keeping is provided by lateral, catenary anchor lines which are attached to the hull near its center of pitch for low dynamic loadings. Several advantages of the classic spar compared with other floating platforms such as tension leg platforms and ship shape hulls are discussed in the literature [2], including structural simplicity, low motions in moderate and extreme ocean waves, good protection of riser connections to the sea bed, and low cost [3]. The concept of Spar as an offshore structure is not new. Spar buoy types of structures have been built before. For example, a floating instrument platform (FLIP) was built in 1961 to perform oceanographic research [4], the Brent Spar was built by Royal Dutch Shell as a storage and offloading platform in the North sea at intermediate water depth [5,6]. Very recently, the first production spar in the world was installed in 1997, at Viosca 826, Gulf of Mexico, the first use of a very large spar in very deep water [7]. Fig. 1 presents a sketch of the structure and its mooring system. In recent years the realization that large spar platforms did offer low cost production options in very deep water has prompted several experimental studies and numerical simulations to obtain a better understanding of their response to dynamical loads. Until now, the publication about the effects of accidental

1 - Professor

2 - Assistant Professor

3 - M .Sc. Student



loads due to underwater explosion causing incident shock wave on a compliant offshore floating platform such as spar are still very limited or not exists. The transient response of a floating structure subjected to underwater explosion is greatly complicated by the detonation of a high explosive, shock wave propagation, bulk and local cavitations, complex fluid–structure interaction phenomena, and the dynamic behaviors of the floating structures. Over the years the UNDEX (UNDERwater EXplosion) response of floating structures was obtained by doing physical testing. Physical testing of a spar platform to determine its response to an underwater explosion is an expensive process that can cause damage to the surrounding environment. The cost involved and the environmental effects require exploration of numerical solution techniques that can analyze the response of a spar platform subject to various explosions. Computational modeling and response, if perfected, can effectively and accurately replace the experimental procedures used to obtain the UNDEX response. This paper addresses a three dimensional analysis of a spar finite element model coupled with a surrounding fluid model subjected to a far-field underwater explosion causing incident shock wave. ABAQUS code [8] was used to conduct the spar shock analysis. The research results on dynamic response to underwater shock would be useful for the improvement of floating structures, enhancement of their resistance to underwater shock and design of spars against time dependent load such as wind, wave, earthquake and similar forces.

Free field problem of Under Water Explosion UNDEX Phenomenon

The general sequence of phenomena that comprise an underwater explosion is understood and good summaries can be found in the literature [9]. The loading mechanisms due to underwater explosion include incident shock wave, free surface reflection wave, bottom reflection wave, gas bubble oscillation and bubble-pulse loading, and bulk and hull cavitations. The shock wave referred here is pressure wave. In brief, the detonation of a high explosive underwater generates a shock wave and a pulsating bubble of detonation product gases. The pulsation of this gas bubble gives rise to the emission of a series of ‘‘bubble pulse’’ pressure waves of decreasing intensity. In general UNDEX divided in two fields, one is near-field and other far-field. In this paper far-field has been considered of significant interest. Any floating structure within the vicinity of an underwater explosion will be subjected to loading from both the shock wave and the bubble pulse pressure waves and will respond according to the strength of these waves and the resilience of the structure. Reflection of the shock wave off the bottom of the ocean is a compression wave that adds additional load to the structure, and the reflection of the shock wave from the free ocean surface causes a reduction in the pressure produced by the shock wave. If the explosion occurs in very close proximity to the structure (near-field) then the dynamics of the bubble are altered and additional target loads come into play [10], otherwise in far-field are not considered, because they are less severe compared to the initial shock wave. Fig. 2 shows the different events occurring during the UNDEX event in a pressure vs. time history plot [11].

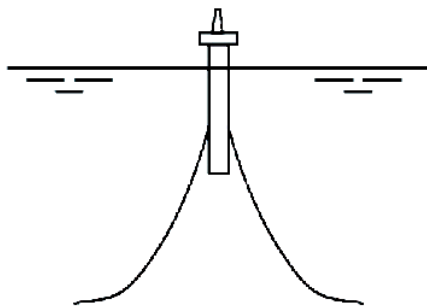


Fig 1- A Spar Platform

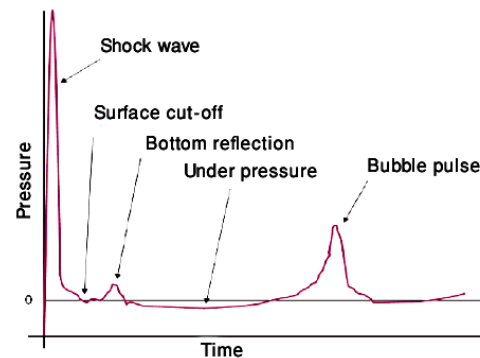


Fig 2- UNDEX Phenomenon

Similitude Relations (Pressure vs. Time)

The pressure vs. time history of an explosive was required for different stand-off distances (distance between the structure and the explosive) to determine pressure shock wave for a spar platform. In this paper the pressure vs. time history at a particular standoff distance from the structure was obtained using the similitude relations [11, 12]. The ‘‘similitude relations’’ equations accurately represent the far-field pressure profiles of an explosive are:

$$P(R, t) = P_c * \left[\frac{a_c}{R} \right]^{1+A} * f(\tau) \quad (1)$$



$$\tau = \left[\frac{a_c}{R} \right]^B * \frac{v_c * t}{a_c} \quad (2)$$

$$\begin{cases} f(\tau) = 0.8251e^{-1.338 \tau} + 0.1749e^{-0.1805 \tau} & , \tau \leq 7 \\ f(\tau) = e^{-\tau} & , \tau \leq 1 \end{cases} \quad (3)$$

Where $P(R,t)$ is the pressure vs. time history, R is the distance from the center of the explosive, a_c is the radius of the spherical charge, $f(a)$ is an exponential decay term, and p_c , v_c , A , and B are the constants which depend on explosive types. Some recommended values obtained from Ref [12] and are shown in Table 1. The shock wave propagation velocity near the charge is 3–5 times of acoustic speed in the water, 1528 m/s. The shock wave profile is inversely proportional to the distance. The shock wave propagation velocity converges rapidly to acoustic wave velocity in the distance of about ten charge radius. Therefore, the far-field spar shock analysis is valid when the standoff distance is at least ten charge radiuses. The linear/acoustic considerations are valid for spar analysis in this range.

Table 1- Material constants for similitude equations

Charge type	P_C, GP_a	$v_C, \text{m/s}$	A	B
TNT (1.52 g/cc)	1.42	992	0.13	0.18
TNT (1.60 g/cc)	1.45	1240	0.13	0.23
TNT (1.60 g/cc)	1.67	1010	0.18	0.185
HBX-1 (1.72 g/cc)	1.71	1470	0.15	0.29
HBX-1 (1.72 g/cc)	1.58	1170	0.144	0.247
Pentolite (1.71 g/cc)	1.65	1220	0.14	0.23

Once the far-field pressure data was obtained from the above relations particular charge, it was applied as a transient load on the spar model.

Pressure Wave Distribution on the Structure

The pressure load acting on the spar due to an underwater explosion changes with respect to both time and space. The pressure vs. time history of an explosive is the relation between pressure acting on the spar, as a spherical or plane wave, at the stand-off point (the point where the wave hits the structure first), and time. In this paper UNDEX wave was modeled as a spherical wave front, which decays exponentially with time. The distribution of this shock wave onto the spar can be considered as a spherical distribution and was obtained using the incident pressure wave equations (IPWE) [8]. IPWE can be written as a separable solution to the scalar wave equation of the form

$$P_I(x_j, t) \equiv P_t(t) P_x(x_j) \quad (4)$$

Where $P_t(t)$ is specified through the pressure vs. time history at the stand-off point x_0 and $P_x(x_j)$ is the spatial variation at a point and is given as:

$$P_x(x_j) = \frac{\|x_s - x_0\|}{\|x_s - x_j\|} \quad (\text{for spherical waves}) \quad (5)$$

$$= 1 \quad (\text{for plane waves}) \quad (6)$$

Where x_s is the specified source point (point of explosion).

By considering the time delay required for the wave to travel from the stand-off point to the point x_j , it is found that,

$$P_I(x_j, t) = P_t\left(t - \frac{R_j - R_o}{c_o}\right) P_x(x_j) \quad (7)$$

$$\equiv P_t(\tau_j) P_x(x_j) \quad (8)$$

And

$$\begin{cases} R_o = \|x_s - x_0\| \\ R_j = \|x_s - x_j\| \end{cases} \quad (\text{for spherical waves}) \quad (9)$$

$$R_j = \frac{|(x_j - x_s) \cdot (x_0 - x_s)|}{\|x_s - x_0\|} \quad (\text{for plane waves}) \quad (10)$$



In Equation (7), c_0 is the wave speed in the fluid, and τ_j is known as the “retarded time” because it includes a shift corresponding to the time required for the wave to move from the stand-off point to x_j .

Fluid–Structure Interaction

Obtaining the response of a spar to an underwater explosion involves integration of the structural behavior and its effects on the surrounding fluid and vice-versa. When the spar is exposed to a shock wave produced by an explosion, the structure deforms and displaces fluid around it. The pressure distribution surrounding the spar structure is also affected by the motion of the spar due to the shock wave. This interaction between the fluid and the structure that exists until the vibration of the system has decayed has to be modeled using coupled fluid-structure equations. In ABAQUS, a surface-based interaction procedure is used to enforce a coupling between the structural surface nodes and the fluid surface nodes. The interaction is defined between the fluid and the spar surface meshes. A detailed explanation of the surface-based interaction procedure is given in Ref. [8]. The reflections of the pressure wave after striking the structure are called scattered waves, which needed to be taken into account while solving the finite element equations. Therefore, the applied load used for solving the finite element equations consisted of the sum of known incident and unknown scattered pressure wave components. The incident wave field is the pressure vs. time history obtained for the explosive. The discretized differential equation for the spar can be expressed as

$$M_s \ddot{u} + C_s \dot{u} + K_s u = \{f(t)\} \quad (11)$$

Where $u(t)$ is the structural displacement vector, M_s and C_s are structural mass, damping matrix respectively and K_s is structural stiffness matrix, $\{f(t)\}$ is the external force vector and a dot denotes temporal derivative. For excitation of a submerged structure by an acoustic wave, $f(t)$ is given by

$$\{f(t)\} = \{-[S_{fs}]^T P\} + \{f_d(t)\} \quad (12)$$

The equations of motion of fluid used in this analysis are of the form

$$M_f \ddot{P} + C_f \dot{P} + K_f P = [S_{fs}] T \quad (13)$$

$$P = (P_I + P_S) \quad (14)$$

Where in equations (12), (13) and (14), $\{f_d(t)\}$ is the applied force vector for the dry-structure, M_f is the mass of fluid, C_f is the fluid damping matrix, K_f is the fluid stiffness matrix, P_I is the incident shock pressure wave, and P_S is the scattered pressure wave. The transformation matrix S_{fs} integrates the fluid and structural degrees of freedoms and was defined on all of the interacting fluid and structural surfaces. The fluid traction T in Equation (13) is the quantity that describes the mechanism by which the fluid drives the solid. By substituting equation (14) into (11) and (12), we obtain the fluid equation in terms of the unknown scattered pressure term. The resulting equation was solved together with Equation (11) to obtain the response of the spar structure.

3-D coupled spar and fluid model

The spar is assumed to be closed at its keel and beam type MPCs are used to tie the end cap (keel) to the hull spar. The cylindrical hull structure has been modeled with S4R shell elements with 6 degrees-of-freedom (i.e. three displacement degrees-of-freedom, i.e. surge, sway and heave along the X, Y and Z axes and three rotational degrees-of-freedom, i.e. roll, pitch and yaw about the X, Y and Z axes). The mesh consists of 6441 nodes (38646 dof) and 6248 elements. The concentrated mass elements were used to represent the total mass of the spar platform such as soft, hard and ballast tanks. Deck structures were modeled with solid elements. The spar hull is made of marine steel with density of 7800 kg/m³, a Young’s modulus of 209.5 GPa, and a Poisson’s ratio of 0.3. The structural material properties assumed to remain linear elastic throughout the process. The spar is entirely floated in water, deep enough so that free surface effects are unimportant and charge offset, and duration of pressure shock wave are selected such that cavitation of the fluid is not significant and no bubble pulse occurs. The finite element spar model, source point, stand-off point, location A, B and C (explained in next section) and co-ordinate system is applied as illustrated in Fig. 3. The external fluid is meshed with 4-node AC3D4 acoustic tetrahedral elements and consists of 2451 nodes and 11080 elements. The fluid is water with a density of 1025 kg/m³, in which the speed of sound is 1528 m/s. The outer boundary of the external fluid is represented by a cylindrical surface. The fact that the fluid is infinite was accommodated in the boundary conditions applied at the outer surface of the fluid. The total horizontal length of the fluid model was 110 m and the vertical length of the fluid domain was 914.4 m. Fig. 4 shows a spar Lagrangian structure in an Eulerian fluid using ABAQUS code.

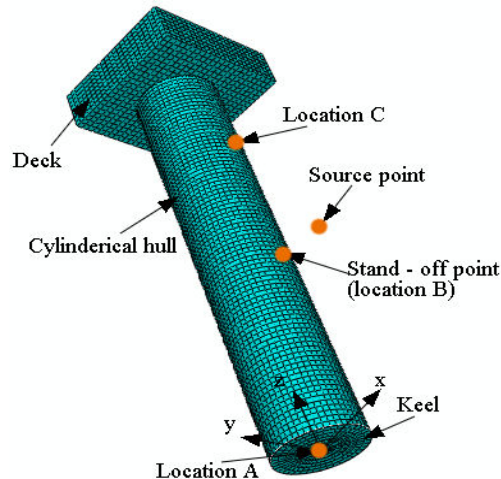


Fig 3- Finite element model of spar platform

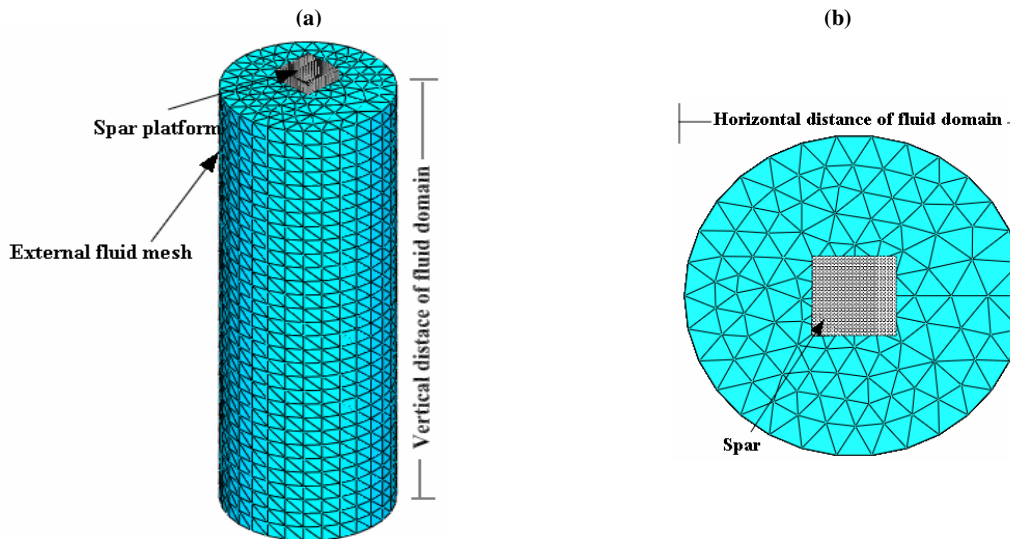


Fig 4- Coupled finite element model of spar and surrounding fluid. (a) 3Ddimensional. (b) Plane

Damping representation

The structural damping matrix is taken to be constant and is dependent on mass and initial stiffness of the structure. The elements of $[C]$ are determined by eq. (15), using the orthogonal properties of $[M]$ and $[K]$, where, ζ is the structural damping ratio ($\zeta=0.05$), ϕ is the modal matrix, ω_i is natural frequency and m_i is the generalized mass

$$\phi^T [C_s] \phi = [2\zeta_i \omega_i m_i] \quad (15)$$

Numerical results and Discussions

The numerical study of spar structure are based on a large spar, which is very similar to the structure installed at the Viosca Knoll 826 field in 914 m water deep and has the same parameters as those used by Weggel et al. [13]. The main particulars of this platform design are: cylindrical hull diameter = 40.5 m; Initial draft = 198.12 m; Length = 214.88 m; Mass(with entrapped water) = 2.6×10^8 kg; Radius of gyration (pitch and roll) = 62.33 m; Distance of CG to buoyancy = 6.67 m; Distance of center of gravity from keel = 92.4 m; Distance of fairleads to keel = 92.6 m; It is assumed that the Spar is connected to the sea floor by four catenary mooring lines placed perpendicular to each other, which are attached to the Spar at the fairleads. In the simulation each of the mooring lines is considered as a non-linear spring with its stiffness taken as 188.733 kN/m up to an offset of 13.7 m and 398.251 kN/m at offsets larger than this. In this paper the interaction between fluid and mooring lines is not considered. The natural period of the spar for the linear response is about 330.89 s for surge, 307.95 s for sway, 70 s for heave, 62.11 s for roll, 62.11s for pitch, 58 s for yaw without accounting for viscous effects. A pressure



shock wave obtained by using simulate equation and produced by a 70 kg HBX-1 explosive charge that is applied on the spar model for a side-on explosion in this paper that shown in Fig. 5.

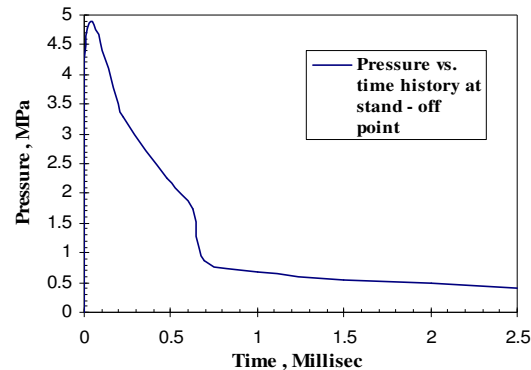


Fig 5- Pressure vs. time history of 70 kg HBX-1 explosive charge

The 70 kg HBX-1 explosive charges (source point) are placed in surge direction at a depth of 99 m from free water surface and located at 35 m from structure surface. Stand-off point is on cylindrical hull structure and placed to distance of 99 m from free water surface. The Explicit model for this UNDEX problem for total active degrees of freedom requires approximately 1GB of memory. The transient analysis is run for 2 seconds with a 5.3×10^{-5} critical time increment. For charges close to the spar, the shock waves propagate as spherical waves moving towards the structure. It is apparent that different portions of the spar will encounter different peak responses, depending on distance from the explosion and angle of attack. To examine the responses for different locations in the spar, three important locations such as center node of keel (location A), stand-off point (location B) and top of the hull structure which is near to free water surface (location C) for this study were chosen which all shown in Fig. 3 and time history of displacement and velocity at these location were obtained. Figs. 6-11 display the displacement and velocity responses at these three locations. Fig. 6-7 indicates that the displacement and velocity responses in the surge, heave and sway directions at center node of keel (location A). Fig. 8-9 represents the displacement and velocity response in the surge, heave and sway directions at stand-off point (location B) and Fig. 10-11 displays the same response at location C. The peck surge direction displacements at $t=2$ s that observed at location B, C were 9.82 And 21.3 cm. In surge displacement direction the incident pressure wave is dampened by the counter balance effect of the structure weight which is illustrates in its curves. Due to the charge being located far away from location A, The results for the keel (location A) are different from the response of location B, C. The peck displacement in this location is low and for surge and sway displacement direction was 2.85 cm and 2.59 cm respectively. The peck heave direction displacement at location A, B, C was 0.057 cm with $t= 1.75$ s, 29 cm with $t= 0.15$ s and 1.7 cm with $t= 2$ s respectively. For all locations, the sway direction had the lowest displacement due to direction of incident wave pressure and such behavior displays an evident difference in the order of displacement in the three directions. The maximum peck of sway velocity direction occurred at location B with 5.15 m/s at 0.15 s. For the location A, B and C the greatest velocity all occurred in the surge direction and were 0.38, 15.2 and 16.9 m/s respectively. At the keel the peak surge velocity are suddenly rising, and the following responses rapidly decline due to effect of scatter pressure wave and geometry of structure oscillation with time.

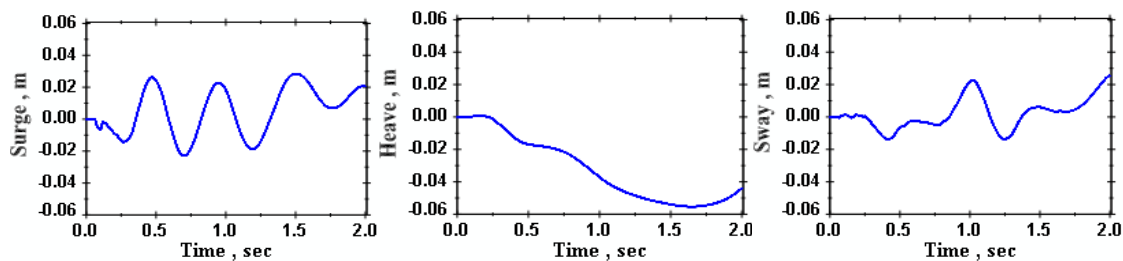


Fig 6- Time history of displacement in surge, heave and sway direction at center node of keel (location A)

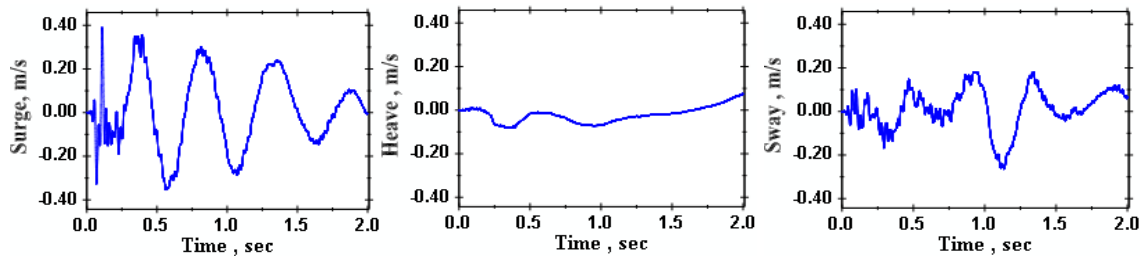


Fig 7- Time history of velocity in surge, heave and sway direction at center node of keel (location A)

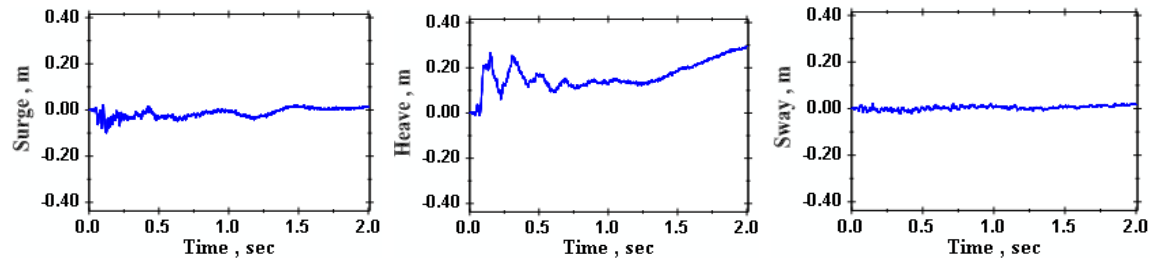


Fig 8- Time history of displacement in surge, heave and sway direction at stand-off point (location B)

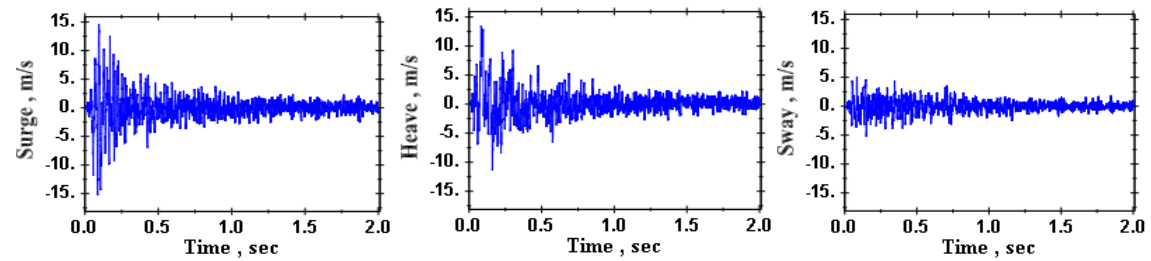


Fig 9- Time history of velocity in surge, heave and sway direction at stand-off point (location B)

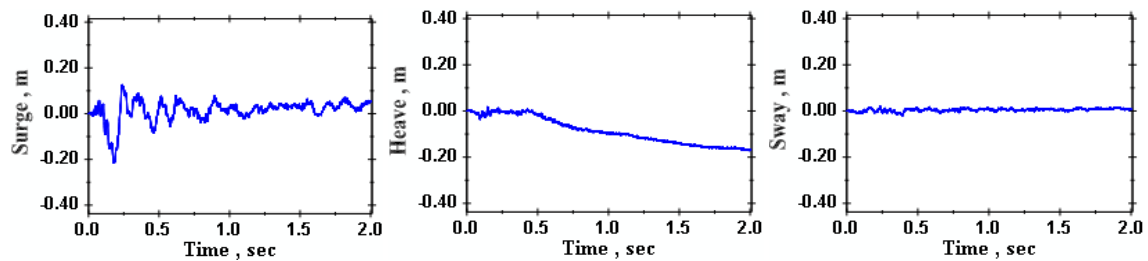


Fig 10- Time history of displacement in surge, heave and sway direction at top of the hull structure (location C)

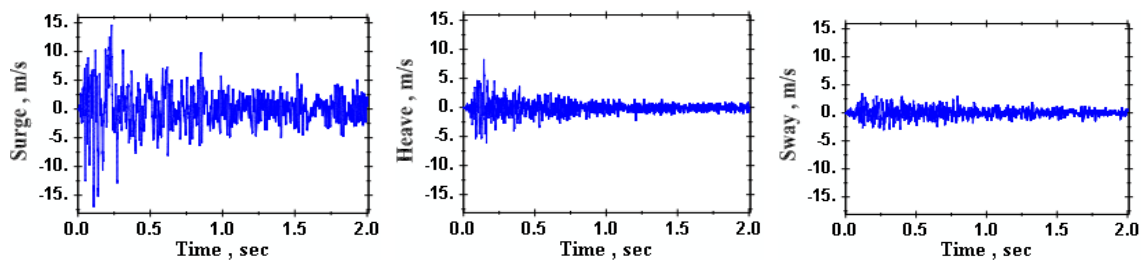


Fig 11- Time history of velocity in surge, heave and sway direction at top of the hull structure (location C)



Important parameters to be considered

For spar platform analysis in general, some considerations must be given to analysis issues: (a) type of analysis to perform, linear or nonlinear, Lagrangian, Eulerian, or coupled Lagrangian–Eulerian, (b) two-dimensional or three-dimensional analysis, (c) modeling techniques, (d) attack geometry, charge size and standoff distance, (e) gas bubble oscillation, (f) bulk and hull cavitation effect, (g) first- and second- order DAA (Doubly Asymptotic Approximation) or surface-based interaction method (h) material properties, etc. There are many more issues to be considered.

Summary and Conclusion

Three-dimensional spar platform shock simulation is performed by modeling the coupled 3-D spar structures and surrounding fluid volume using the ABAQUS code. The spar shock simulation conducted in this paper clearly demonstrates that three-dimensional full spar shock modeling and simulation can be achieved based on the state-of-the-art technologies and computer hardware. This investigation developed a procedure to analyse the shock response at different locations. It employed the explicit finite element method coupled with the surface based interaction method to study the transient dynamic response of a 70 kg HBX-1 subjected to an underwater explosion. Consequently, the shock loading history at the hull structure, velocity and displacement time history at different locations are presented in detail. Based on the results, we can conclude that in most cases, the equipment is more sensitive than the structure to shock, and damage may be caused by higher acceleration or displacement. When the spar was subjected to underwater shock, typical velocity and displacement time histories were obtained. These results should confirm whether the specification requirements were satisfied or not. This work represents a preliminary study of the transient responses of a spar platform under shock loading. It aims to assist in the choice of structure and equipment to ensure durability in a shock environment, improvement of floating structures, enhancement of their resistance to underwater shock and design of spars against time dependent load such as wind, wave, earthquake and similar forces. The gas bubble effect and shock resistant design of spar structure and attached equipment are merit further study.

References

1. Converse, R. and Bridges, R. (1996) Adapting Gulf of Mexico spars to the west of Shetland. *Floating Production Systems conference*, IBC Technical Services, London.
2. Vardeman, R.D., Richardson, S. and McCandless, C.R. (1997) Neptune project: overview of project management. OTC.
3. Ma, Q.W. and Patel, M.H. (2001) On the non-linear forces acting on a floating spar platform in ocean waves. *International Journal of Appl Ocean Res*, **23**, 29– 40.
4. Fisher, F.H. and Spiess, F.N. (1963) Flip floating instrument platform. *Journal of the Acoustical Society of America*. **35** (10), 1633–1644.
5. Bax, J.D. and de Werk, K.J.C. (1974) A floating storage unit designed specially for the Severes Environmental Conditions. Society of Petroleum Engineers (SPE paper 4853).
6. Van Santen, J.A. and de Werk, K. (1976) On the typical qualities of spar type structures for initial or permanent field development. In: *Offshore Technology Conference* (OTC-2716), pp. 1105–1118.
7. Glanville, R.S., Halkyard, J.E., Davies, R.L., Steen, A. and Frimm, F. (1997) Neptune Project: Spar history and design consideration s. OTC 8382, *Offshore Technology Conference*, Houston, TX, USA, Vol. 2, 237 ± 51.
8. ABAQUS Theory Manual, Version 6.4.1. Hibbitt, Karlsson, and Sorensen, Inc., Pawtucket, RI, 2003.
9. Snay HG. Hydrodynamics of underwater explosions. In: *Symposium on naval hydrodynamics, Publication 515. Washington, DC*: National Academy of Science, National Research Council; p. 325–52.
10. M. Brett, J. and Yiannakopoulos, G. (2007) A study of explosive effects in close proximity to a submerged cylinder. *International Journal of Impact Engineering*, Available online at www.sciencedirect.com
11. Coles, R. H. (1948) *Underwater Explosions*, Princeton University Press, Princeton.
12. Geers, T. L. and Hunter, L. S. (2002) An Integrated Wave-Effects Model for an Underwater Explosion Bubble. *Journal of Acoustical Society of America*, **4**, 1584-1601.
13. Weggel, D.C. and Roesset, J.M. (1996) Second-order dynamic response of a large spar platform: numerical predictions versus experimental results. *OMAE'96*, Florence, Italy. Vol. 1, Part A, p. 489 ±96.